

Comparison of the Native CCMV Virion with *in Vitro* Assembled CCMV Virions by Cryoelectron Microscopy and Image Reconstruction

James M. Fox,^{*1} Guoji Wang,^{†2} Jeffrey A. Speir,^{‡3} Norm H. Olson,[†] John E. Johnson,[†] Timothy S. Baker,[†] and Mark J. Young^{*4}

^{*}Department of Plant Pathology, Montana State University-Bozeman, Bozeman, Montana 59717; [†]Department of Biological Sciences, Purdue University, West Lafayette, Indiana 47907; and [‡]Department of Molecular Biology, Scripps Research Institute, La Jolla, California 92037

Received January 6, 1998; returned to author for revision February 2, 1998; accepted February 25, 1998

Cryoelectron microscopy and three-dimensional image reconstruction analysis has been used to determine the structure of native and *in vitro* assembled cowpea chlorotic mottle virus (CCMV) virions and capsids to 25-Å resolution. Purified CCMV coat protein was used in conjunction with *in vitro* transcribed viral RNAs to assemble RNA 1 only, RNA 2 only, RNA 3/4 only, and empty (RNA lacking) virions. The image reconstructions demonstrate that the *in vitro* assembled CCMV virions are morphologically indistinguishable from native virions purified from infected plants. The viral RNA (vRNA) is packaged similarly within the different types of virions. The centers of all assembled particles are generally devoid of density and the vRNA packs against the interior surface of the virion shell. The vRNA appears to adopt an ordered conformation at each of the quasi-threefold axes. © 1998 Academic Press

Key Words: CCMV; virus assembly; cryoelectron microscopy.

INTRODUCTION

Cowpea chlorotic mottle virus (CCMV) is a member of the Bromoviridae family of viruses (alphavirus-like superfamily). The bromovirus group has three members: CCMV, brome mosaic virus, and broad bean mottle virus. The bromoviruses have 28-nm icosahedral capsids which separately encapsidate four, positive sense, single-stranded viral RNAs (vRNAs) into three structurally similar virions (for reviews see Ahlquist, 1992; Bancroft and Horne, 1977; Lane, 1981). RNA 1 (3171 nucleotides in length) and RNA 2 (2774 nucleotides in length), which encode for proteins involved in RNA-dependent RNA replication, are packaged in separate virions. RNA 3 (2173 nucleotides in length; a mRNA for the 32-kDa viral movement protein) and RNA 4 (824 nucleotides in length; a subgenomic RNA expressed from RNA 3 which serves as the mRNA for the 20-kDa coat protein) are copackaged into a third particle in an approximate 1:1 molar ratio (Loesch-Fries and Hall, 1980). All three virions are required to establish infection of a plant cell.

The bromoviruses, and CCMV in particular, provide

an ideal system for examining the protein–protein and protein–RNA interactions that dictate icosahedral virus assembly, stability, and disassembly (Fox *et al.*, 1994; Zhao *et al.*, 1995). CCMV has been used as a model system for viral assembly ever since Bancroft and Hiebert first demonstrated that purified RNA and coat protein can reassemble *in vitro* to produce infectious virions (Bancroft *et al.*, 1968, 1969; Bancroft and Hiebert, 1967; Hiebert and Bancroft, 1969; Hiebert *et al.*, 1968). One unique aspect of the CCMV *in vitro* disassembly/assembly system is that a wide range of polymorphic forms of the virion assemble in varied chemical environments (Bancroft *et al.*, 1968, 1969; Bancroft and Hiebert, 1967; Hiebert and Bancroft, 1969; Hiebert *et al.*, 1968; Johnson and Speir, 1997). This suggests that changes in ionic strength, pH, and temperature can effect both the protein–protein and protein–RNA interactions in virion assembly and disassembly.

CCMV is stable at pH 5.0 and sediments as 88-S virions in sucrose density gradients. Increasing the pH to >7.0 and maintaining a low ionic strength ($I = 0.1$) induces swelling of the virion by approximately 10% and changes the sedimentation value to 78 S. Swelling is a result of a radial expansion of the virion at the quasi-threefold axes (Fig. 1), which produces 20-Å openings at each of these axes (Speir *et al.*, 1995). Presumably swelling only occurs when Ca^{2+} , which binds to the capsid at these axes, is first removed. The swelling process can be reversed by adding divalent cations back (i.e., Mg^{2+} , Ca^{2+}), or by lowering the pH. The role, if any, of swelling

¹Present address: Rocky Mountain Laboratories-LPVD, NIAID/NIH, Hamilton, MT 59840.

²Present Address: Department of Pathology, University of Pittsburg, Pittsburg, PA 15261.

³Present Address: Department of Molecular Biology, Scripps Research Institute, La Jolla, CA 92037.

⁴To whom correspondence and reprint requests should be addressed. Fax: (406) 994-1848. E-mail: uplmy@gemini.oscs.montana.edu.

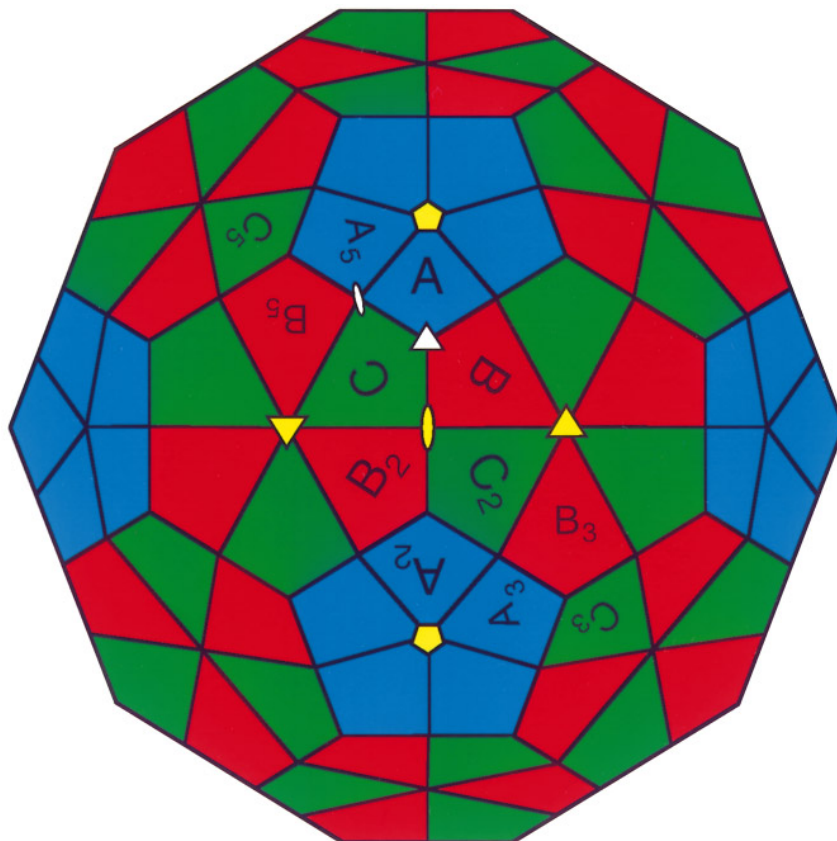


FIG. 1. A truncated icosahedral model of CCMV. Positions of the icosahedral rotational axes are marked by yellow symbols (pentagons, fivefold rotational axes; triangles, threefold rotational axes; ovals, twofold rotational axes). The quasi-threefold and quasi-twofold axes are indicated by the white triangle and white oval, respectively. The polygons represent chemically identical protein subunits which represent the three slightly different geometrical (chemical) environments of the coat protein. This is indicated by their different coloring.

is unknown, though it has been postulated that it may play a role in the cotranslational disassembly of virions *in vivo* (reviewed in Albert *et al.*, 1997; Heaton and Morris, 1992; Verduin, 1992).

Rapid lowering of the pH and ionic strength (<5.5 and $I = 0.1$, respectively) causes free coat protein to form 52-S empty capsids (Bancroft *et al.*, 1968). Formation of empty capsids is strictly an *in vitro* effect because such particles have not been observed in natural infections. Nevertheless, this property provides a novel system for distinguishing the roles that protein-protein and protein-RNA interactions contribute to virus assembly and structure. Under appropriate conditions (pH = 7.4, $I < 0.05$), CCMV virions containing RNA can be reassembled *in vitro* from purified coat protein and vRNA (Zhao *et al.*, 1995). The *in vitro* assembled virions are infectious and, with electron microscope, appear similar to plant-purified virions.

The structure of CCMV was recently determined to high resolution by means of X-ray crystallography (Speir *et al.*, 1995). The CCMV structure exhibits several features not previously seen in other plant viruses. The quaternary structure of CCMV displays a $T = 3$, quasi-symmetry with 32 prominent capsomers. The capsomers

occur as 12 pentamers and 20 hexamers assembled from the 20-kDa coat protein (Fig. 1). Each coat protein subunit is comprised of an eight-stranded, anti-parallel, β -barrel core, with minimal insertions between the β -sheet strands. The core structure is quite similar to that found in many other small, spherical plant and animal viruses (Harrison, 1990; Johnson and Speir, 1997; Rossmann and Johnson, 1989). Extending in opposite directions away from the β -barrel core are the C-terminal and N-terminal arms of the coat protein. The pentameric and hexameric capsomers of the virion are linked through C-terminal extensions originating from two coat proteins, one from each type of capsomer. The C-terminal extension from one coat protein subunit extends across the twofold axis of the virion and invades the adjacent coat protein subunit. The N-terminal arm from the adjacent subunit provides support and "clamps" the invading C-terminal arm. In addition to providing the clamp, the N-terminal extensions of the threefold related coat proteins converge at the threefold axes of the virion and intertwine to form a hexameric tubular structure (β -hexamer) beneath the contiguous protein shell. The β -hexamer is a principal stabilizing factor in the virion (Speir *et al.*, 1995; Zhao *et al.*, 1995). Five N-terminal arms

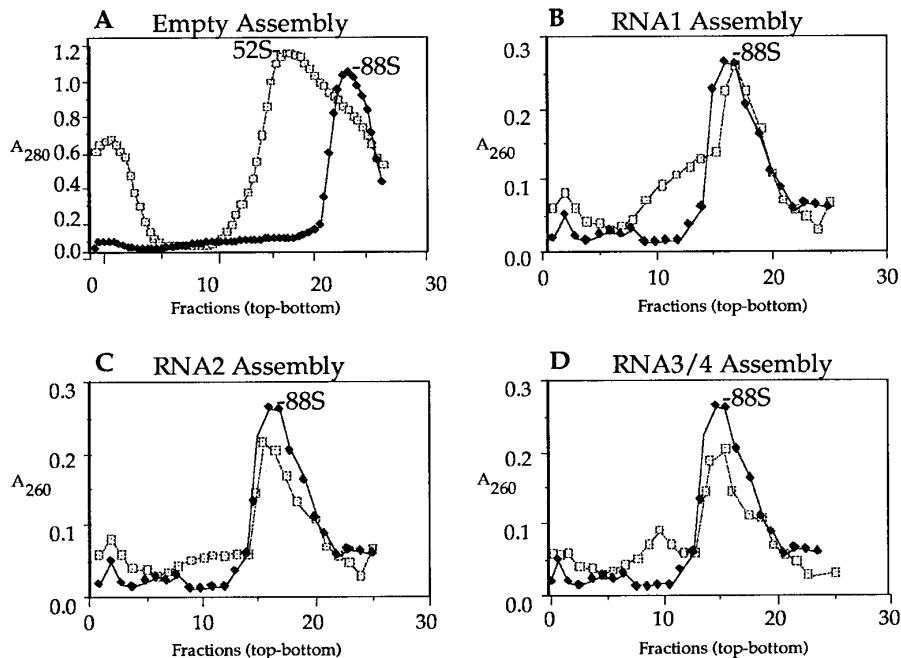


FIG. 2. Sucrose gradient profiles of *in vitro* assembled CCMV particles (□) used for cryoelectron microscopy and image reconstructions. (A) Empty particles devoid of vRNA. (B) RNA 1-containing particles. (C) RNA 3-containing particles. (D) RNA 3/4-containing particles. S values and the profile of native virus purified (◆) from infected plants are indicated in each gradient.

also extend toward each icosahedral fivefold axis, but they do not form a similar β -annulus structure. The N- and C-terminal extensions provide an intricate network of "ropes" that "tie" subunits together.

The combination of high resolution structure and an *in vitro* assembly system makes CCMV an attractive system for examining virus assembly. Our goals were to determine if virions assembled *in vitro* are structurally similar to plant-purified virions and to determine the structural similarities between RNA-containing virions and empty virions. In addition, we set out to examine the differences that might exist between the separate RNA-containing CCMV virions. Low resolution electron microscopy studies have suggested that the separate virions were structurally similar. In this paper we report a cryoelectron microscopy and three-dimensional image reconstruction analysis of the structures of plant-purified CCMV virions, *in vitro* assembled empty capsids, and three different *in vitro* assembled RNA containing virions.

RESULTS

Isolation of native CCMV virions from plants

Purified native virions from infected plants sediment as 88-S particles on the sucrose gradients as expected (Fig. 2).

In vitro assembly of empty capsids

Empty CCMV capsids were assembled *in vitro* from purified CCMV coat protein. Under conditions of high

ionic strength and low pH buffer ($I = 1.0$, pH 4.8), the coat protein assembles into empty capsids. The empty capsids sediment slower (52 S) than native virions (88 S) (Fig. 2).

In vitro assembly of individual RNA containing virions

RNA containing virions were assembled *in vitro* using purified CCMV coat protein and vRNAs transcribed *in vitro* from CCMV cDNA clones. The assembly of RNA 1 and RNA 2 containing virions was accomplished using a 5:1 (wt/wt) ratio of CCMV coat protein to *in vitro* transcribed RNA. Using proper ionic strength and pH conditions ($I = 0.1$, pH = 7.0), virions were assembled that were structurally similar to native virions as determined by transmission electron microscopy (Fig. 3). In addition, *in vitro* assembled virions sedimented similarly to native virions in sucrose gradients (Fig. 2). The integrity of the packaged RNA was postassembly analyzed by gel electrophoresis and was determined, mainly, to be full-length RNA (data not shown). This indicated that RNA degradation was not occurring during the assembly of virions and that the RNA within the virions was full-length.

The assembly of RNA 3- and 4-containing virions was accomplished using an alternative approach. For both RNA 1- and RNA 2-containing virions, only one type of RNA was present in the assembly reaction and therefore only one type of RNA could be packaged into virions. In addition, owing to the size of these RNAs, only one molecule of either RNA 1 or RNA 2 can be packaged into a virion. However, because RNA 3 and 4 are of a smaller

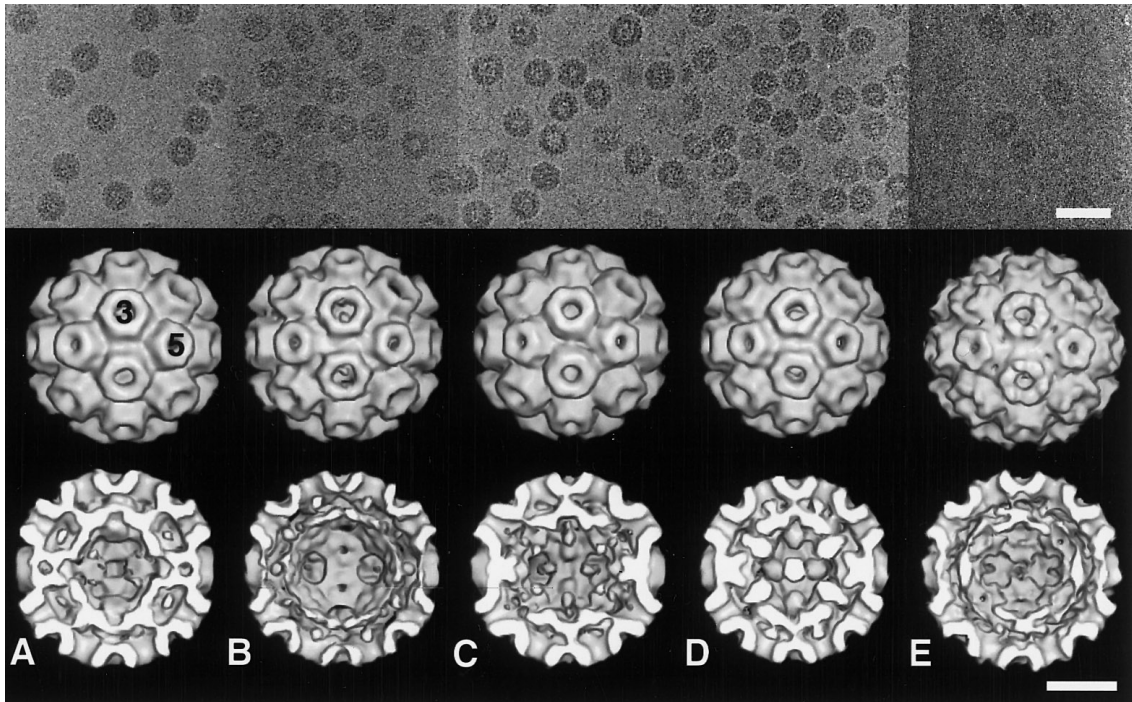


FIG. 3. Cryoelectron microscopy and three-dimensional image reconstructions of plant-purified native particles and *in vitro* assembled CCMV particles. The top panel shows electron micrographs of frozen-hydrated (A) native, (B) empty, (C) RNA 1, (D) RNA 2, or (E) RNA 3/4 particles assembled *in vitro*. The middle panel shows shaded, surface representations of native particles or *in vitro* assembled empty, RNA 1, RNA 2, or RNA 3/4 particles. The three- and five-fold icosahedral axes are indicated on the native particles. All particles are shown in the same orientation. Top bar, 50 nm. Bottom bar, 10 nm.

size, a series of different virion types could be produced: virions containing two molecules of RNA 3, two molecules of RNA 4, three molecules of RNA 4, or one molecule of RNA 3 and one molecule of RNA 4 (the native form). To favor formation of native RNA 3/4 virions, we had to optimize the ratio of RNA 3 to RNA 4 in the assembly. Several RNA 3/4 ratios were tested and the optimal ratio to obtain RNA 3/4 virions was determined to be 1:2 RNA 3 to RNA 4 (data not shown). Using RNA 3 and RNA 4 in this ratio produced virions that resembled native virions (Fig. 3) and sedimented similarly to native virions on sucrose gradients (Fig. 2). Postassembly analysis of the packaged RNA indicated that the two RNA species were primarily full-length and present in an approximate ratio of 1:1 as determined by Northern blot analysis (Fig. 4).

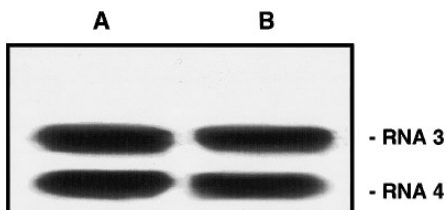


FIG. 4. Northern blot hybridization of (A) native CCMV virions and (B) *in vitro* assembled CCMV RNA 3/4-containing particles.

Cryoelectron microscopy and image reconstruction of virions

Electron micrographs of CCMV virions embedded in vitreous ice (Fig. 3) provided particle images from which three-dimensional density maps were computed to 25-Å resolution.

The image reconstruction of native CCMV revealed a number of features consistent with the X-ray structure (Speir *et al.*, 1995). Thirty-two doughnut-like capsomers are present on the exterior surface of the virion (Fig. 3). These capsomers extend above the contiguous protein shell and clearly exhibit both pentameric and hexameric morphologies. Density inside the virion has been assigned to the viral RNA (Speir *et al.*, 1995). The RNA primarily coats the inner surface of the protein shell, with little or no density found in the center of the virion. The highest density attributed to RNA occurs at the B-C coat protein interface and extends toward the quasi-threefold axis of the virion (Fig. 1).

The image reconstruction of the empty CCMV virion is remarkably similar to native CCMV in the exterior portions of the structure (Fig. 3). Like native CCMV, defined pentameric and hexameric capsomers are present on the virion surface. As expected, the interior of the empty capsid is devoid of density attributable to RNA, though some density does exist at each of the threefold axes

inside the shell. This density might be attributed to the N-terminal extensions of the coat protein that extend toward the virion interior and normally interact with viral RNA in native virions.

The image reconstructions of *in vitro* assembled RNA-containing virions, like empty virions, show that all particle types have very similar exterior morphologies (Fig. 3). Slight differences occur in the interior of each nucleocapsomer. These differences may reflect the distinct sizes of the RNA species and differences in the packaged structures. Strong RNA density at each of the quasi-threefold axes and weaker RNA density at each of the five-fold axes is common to each type of virion. Like native CCMV, the center of each *in vitro* RNA-containing particle is devoid of density.

DISCUSSION

The utility of the *in vitro* assembly system for producing a wide range of CCMV particles is well documented (Bancroft *et al.*, 1969; Johnson and Speir, 1997). However, the dependability of the *in vitro* assembly system to produce virions that are indistinguishable from plant-purified virions had been previously impossible to determine. Our study has demonstrated that virions assembled *in vitro* are structurally identical to native virions to 25-Å resolution. We have demonstrated for the first time that the protein shell of empty particles assembled *in vitro* are structurally identical to the protein shell of native or *in vitro* assembled RNA-containing virions. These results further validate the utility of *in vitro* assembly system to accurately mimic CCMV assembly *in vivo*. Our results additionally support the notion that CCMV virion assembly is dictated solely by the coat protein and viral RNA and that no additional factors are likely to be required for proper assembly *in vivo*. However, our results do not eliminate the possibility that additional factors may play a role *in vivo*.

Plant-purified virus is comprised of three different types of RNA-containing virions. Therefore, image reconstructions of native CCMV samples would normally lead to a structure that is an average of all three virion types. The high noise level in each individual particle image makes it impossible with present technology to distinguish the three different virion types in a mixed sample. Thus, it was necessary to compute separate image reconstructions of each type of virion to determine if significant structural differences existed between them. The *in vitro* assembly of each type of RNA (from *in vitro* transcribed cDNA)-containing virion was the most feasible approach to obtain these virions.

Though the assembly of CCMV *in vitro* has been performed many times, the techniques employed have led to the formation of minor amounts of aberrant virion structures in addition to properly assembled virions. For the cryo-TEM studies, it was imperative to have high quality,

homogenous samples. Hence, we modified previous protocols to enhance the production of homogenous virion preparations. For example, more efficient virion assembly occurs when the pH is increased and the ionic strength is kept low ($I < 0.05$ M). The optimal protein:RNA ratio for RNA-containing virions was found to be 5:1 (wt:wt). Partially assembled virions, which resulted at lower protein:RNA ratios, would assemble into complete virions upon the addition of more coat protein (data not shown). These results indicate that, at pH 7.0, one favors protein–RNA interactions compared to protein–protein interactions.

Conditions for assembling RNA 3/4 virions *in vitro* were more difficult to produce because standard procedures led to production of RNA 3 only and RNA 4 only, as well as RNA 3/4-containing virions. The optimal assembly conditions include twice as much RNA 4 as RNA 3. In fact, this is the same ratio of these RNA species observed during the late stage of infection of plant cells when virion assembly occurs (Loesch-Fries and Hall, 1980). Two possibilities exist to explain the coencapsulation of RNA 3 and RNA 4 within a single virion. The first possibility is that there is an upper size limit of RNA that can be packaged within a CCMV virion and RNA 3 and RNA 4 together approximately equal this size. The added size of RNA 3 and RNA 4 (2900 nt) approximately equals that of RNA 1 (3100 nt) or RNA 2 (2900 nt). Alternatively, it may be that RNA 3 and RNA 4 dimerize and each dimer might initiate virion assembly. Precedence for this exists in the hepatitis virus and HIV systems where viral RNA dimerization is required for virion assembly.

Empty virions are not produced in the natural infection process. Intracellular pH conditions are generally close to neutral. Under such conditions *in vitro*, viral RNA is required to get coat protein to assemble into virions. However, purified samples of coat protein will assemble into capsids in the absence of RNA if the pH is rapidly lowered to 5.0 under high ionic strength conditions. Presumably, the combination of low pH and high ionic strength alleviates repulsive electrostatic charges in the coat protein that are normally neutralized by the viral RNA. However, the kinetics of capsid formation is influenced by the RNA. Though no quantitative data exist, qualitative observations have shown that virion assembly occurs immediately upon adding protein and RNA together, whereas significant formation of capsids only occurs after several minutes. In addition, assembled empty capsids are unstable because they disassemble if the pH is increased slightly ($> \text{pH } 6.0$).

The cryo-TEM and crystal structures of CCMV virions appear remarkably identical at 25-Å resolution. The high resolution crystal structure reveals that the hexameric capsomers are stabilized by six N-terminal arms, one from each coat protein subunit at the three-fold axis, that form a cylindrical β -sheet structure called a β -hexamer

(Speir *et al.*, 1995). No such interaction is observed at the five-fold axis.

At 25 Å resolution, it is not possible to distinguish with certainty, the RNA from protein density in image reconstructions of nucleocapsids. This is particularly true in regions where RNA and protein interact. However, in empty capsids the N-terminal regions of the coat protein should be visible in the interior of particles if these regions are not highly disordered. Density is observed at low radii at each of the three-fold axes of the empty capsid, but not observed at the five-fold axes. Hence, the N-termini extensions are likely disordered at the five-fold axes whereas they adopt a stable (ordered) structure at the three-fold (quasi-sixfold) positions.

Comparison of the full and empty particle structures indicates that the viral RNA lies next to the inner surface of the protein shell and very little, if any, is present in the center of virions. Highly ordered RNA density also occurs at each of the quasi-threefold axes. The density at the quasi-threefold axes is very strong compared to that at the fivefold axes. In the crystal structure, ordered RNA is also observed at each of the B-C coat protein subunit interfaces and extends towards the quasi-threefold axes. This ordered RNA which composes approximately 20% of the viral RNA may stabilize virions by providing strong protein–RNA interactions. Under conditions which cause CCMV virions to swell, the capsid expands at the quasi-threefold axes and this leads to the formation of 20-Å diameter holes in the virus shell at these positions. It is the protein–RNA interactions maintained at these axes which prevent swollen virions from disassociating. Empty capsids can not swell without disassociating, presumably because there is no RNA to stabilize the capsid against disassembly. In addition to providing stability, the RNA at the quasi-threefold axes may have an important role during virion assembly. When RNA is absent CCMV coat protein can assemble into hexameric sheets *in vitro*. We postulate that vRNA along with Ca²⁺ induces curvature of the growing capsid at the quasi-threefold axes and this promotes the formation of spheres rather than sheets.

Our working hypothesis is that the RNA near the five-fold axes interacts with the N-terminal extensions of the pentamer coat protein subunits. These N-terminal extensions are not “locked” in place like the ones at the threefold axes that form the β-hexamer structure. Thus, the N-termini at the fivefold axes are likely very dynamic structures and may reversibly move in and out of the virion. The fact that this region of the coat protein is not resolved in either the crystal structure or the image reconstruction supports its dynamic nature. Recent work (Albert *et al.*, 1997) has implicated the fivefold axes as the initiation site of virion disassembly. Our model predicts that at the fivefold axes, five N-terminal extensions of the coat proteins become externalized and form a five-helix bundle that acts as channel or pore for the extrusion of

the viral RNA via a cotranslational disassembly process. Presumably vRNA at the fivefold axes in contact with the N-termini of the coat protein subunits might be pulled to the exterior of the virion as a consequence of channel formation. The model predicts that the trigger for channel formation is a change in pH.

MATERIALS AND METHODS

Virus propagation and purification

Cowpea chlorotic mottle virus (type strain) was propagated in *Vigna unguiculata* (queens blackeye) as previ-

purified CCMV coat protein (in buffer B) and CCMV RNA. The mixture was dialyzed against RNA assembly buffer (50 mM NaCl, 50 mM Tris-HCl, pH 7.2, 10 mM KCl, 5 mM MgCl₂, 1 mM DTT) for 12 h at 4°C. For CCMV RNA 1 and RNA 2 virions, the ratio of coat protein to RNA used was 5:1 (wt/wt). In the assembly of CCMV RNA 3/4 virions, a coat protein to RNA ratio of 5:1 (wt/wt) was used where the RNA fraction was 1:2 RNA 3 to RNA 4 (wt/wt). The assembly reactions were collected and washed with RNA assembly buffer using Centricon-100s as described for the empty capsids. Virus buffer (0.1 M sodium acetate, pH 4.8, 1 mM EDTA, 1 mM sodium azide) was used for the final wash to stabilize the virions for storage. Virions were concentrated to a range of 0.2–1.0 mg/ml for electron microscopy.

Electron microscopy and image reconstruction

The cryoelectron microscopy and image processing procedures used to obtain three-dimensional reconstructions of CCMV particles have been previously described (Baker *et al.*, 1988; Cheng *et al.*, 1994a, 1994b; Zhao *et al.*, 1995). The *in vitro* assembled CCMV virions were examined in a Philips EM420 (Philips Electronic Instruments, Mahwah, NJ) transmission electron microscope and maintained at near liquid nitrogen temperature in a Gatan cryotransfer stage (Gatan Inc., Warrendale, PA). The vitrified, native sample was examined in a Philips CM12 electron microscope and micrographs were recorded with a spotscan procedure (Downing and Glaeser, 1986). The micrographs of the *in vitro* assembled virion samples chosen for image processing were recorded under minimal dose conditions (~2000 e⁻/nm²) at an instrument magnification setting of 49,000×, at 80 kV, and at an objective lens defocus of 0.9 μm. The orientations and phase origins (centers) of the particle images were determined by use of a model-based approach which utilizes a reconstruction of native CCMV as the starting model (Baker and Cheng, 1996; Cheng *et al.*, 1994a, 1994b; Speir *et al.*, 1995). The total number of particles of each image reconstruction was 37 for plant-purified native virions, and 23 (empty capsids), 30 (RNA 1 virions), 32 (RNA 2 virions), and 50 (RNA 3/4 virions) for *in vitro* assembled particles.

ACKNOWLEDGMENTS

This work was supported by the National Science Foundation grants MCB 9723752 to M.Y. and MCB9206305 to T.S.B.

REFERENCES

- Ahlquist, P. (1992). Bromovirus RNA replication and transcription. *Curr. Opin. Gen. Dev.* **2**, 71–76.
- Albert, F., Fox, J., and Young, M. J. (1997). Virion swelling is not required for cotranslational disassembly of cowpea chlorotic mottle virus. *J. Virol.* **71**, 4296–4299.
- Allison, R., Janda, M., and Ahlquist, P. (1988). Infectious *in vitro* transcripts from cowpea chlorotic mottle virus cDNA clones and exchange of individual RNA components with brome mosaic virus. *J. Virol.* **62**, 3581–3588.
- Baker, T. S., and Cheng, R. H. (1996). A model-based approach for determining orientations of biological macromolecules imaged by cryo-electron microscopy. *J. Struct. Biol.* **116**, 120–130.
- Baker, T. S., Drak, J., and Bina, M. (1988). Reconstruction of the three-dimensional structure of simian virus 40 and visualization of the chromatin core. *Proc. Natl. Acad. Sci. USA* **85**, 422–426.
- Bancroft, J. B., Bracker, C. E., and Wagner, G. W. (1969). Structures derived from cowpea chlorotic mottle and brome mosaic virus protein. *Virology* **38**, 324–335.
- Bancroft, J. B., and Hiebert, E. (1967). Formation of an infectious nucleoprotein from protein and nucleic acid isolated from a small spherical virus. *Virology* **32**, 354–356.
- Bancroft, J. B., and Horne, R. W. (1977). Bromovirus (brome mosaic virus) group. In "The Atlas of Insect and Plant Viruses" (K. Maramorosch, Ed.), Vol. 8, pp. 287–302. Academic Press, New York.
- Bancroft, J. B., Wagner, G. W., and Bracker, C. E. (1968). The self-assembly of a nucleic-acid free pseudo-top component for a small spherical virus. *Virology* **33**, 146–149.
- Cheng, R. H., Kuhn, R. J., Olson, N. H., Rossmann, M. G., Choi, H. K., Smith, T. J., and Baker, T. S. (1994a). Nucleocapsid and glycoprotein organization in an enveloped virus. *Cell* **80**, 621–630.
- Cheng, R. H., Reddy, V. S., Olson, N. H., Fisher, A. J., Baker, T. S., and Johnson, J. E. (1994b). Functional implications of quasi-equivalence in a T = 3 icosahedral animal virus established by cryo-electron microscopy and x-ray crystallography. *Structure* **2**, 271–282.
- Downing, K. H., and Glaeser, R. M. (1986). Improvement in high resolution image quality of radiation-sensitive specimens achieved with reduced spot size of the electron beam. *Ultramicroscopy* **20**, 269–278.
- Fox, J. M., Johnson, J. E., and Young, M. J. (1994). RNA/protein interactions in icosahedral virus assembly. *Semin. Virol.* **5**, 51–60.
- Harrison, S. C. (1990). Common features in the structures of some icosahedral viruses: A partly historical overview. *Virology* **1**, 387–403.
- Heaton, L. A., and Morris, T. J. (1992). Structural implications for spherical plant virus disassembly *in vivo*. *Virology* **3**, 433–439.
- Hiebert, E., and Bancroft, J. B. (1969). Factors affecting the assembly of some spherical viruses. *Virology* **39**, 296–311.
- Hiebert, E., Bancroft, J. B., and Bracker, C. E. (1968). The assembly *in vitro* of some small spherical viruses, hybrid viruses, and other nucleoproteins. *Virology* **34**, 492–508.
- Johnson, J. E., and Speir, J. A. (1997). Quasi-equivalent viruses: A paradigm for protein assemblies. *J. Mol. Biol.* **269**, 665–675.
- Lane, L. C. (1981). The Bromoviruses. In "Handbook of Plant Virus Infection and Comparative Diagnosis" (E. Kurstak, Ed.). Elsevier/North-Holland, Amsterdam.
- Loesch-Fries, L. S., and Hall, T. C. (1980). Synthesis, accumulation and encapsidation of individual brome mosaic virus RNA components in barley protoplasts. *J. Gen. Virol.* **47**, 323–332.
- Rossmann, M. G., and Johnson, J. E. (1989). Icosahedral RNA virus structure. *Annu. Rev. Biochem.* **58**, 533–573.
- Sambrook, Fritsch, E. F., and Maniatis, T. (1989). In "Molecular Cloning: A Laboratory Manual, 2nd ed." Cold Springs Harbor Laboratory Press, Cold Spring Harbor, NY.
- Speir, J. A., Munshi, S., Wang, G., Baker, T. S., and Johnson, J. E. (1995). Structures of the native and swollen forms of cowpea chlorotic mottle virus determined by X-ray crystallography and cryo-electron microscopy. *Structure* **3**, 63–78.
- Verduin, B. J. M. (1992). Early interactions between viruses and plants. *Semin. Virol.* **3**, 423–431.
- Zhao, X., Fox, J. M., Olson, N. H., Baker, T. S., and Young, M. J. (1995). *In Vitro* assembly of cowpea chlorotic mottle virus from coat protein expressed in *Escherichia coli* and *in vitro*-transcribed viral cDNA. *Virology* **207**, 486–494.